Spatially Controlled Molecular Encapsulation in Natural Pine Pollen Microcapsules

Arun Kumar Prabhakar, Michael G. Potroz, Soohyun Park, Eijiro Miyako,* and Nam-Joon Cho*

The loading of multiple drugs into a single carrier is an effective advanced clinical therapeutic for various diseases. Here, by exploiting the architectural features of natural pine pollen from *Pinus massoniana*, the spatially controlled encapsulation of two types of molecules in distinct compartments of a single microparticulate carrier is demonstrated. By simple vacuum and passive loading, diverse molecules such as proteins, organic dyes, and a drug are effectively encapsulated into the pollen microcapsule in binary fashion. This technique represents an advancement toward the use of natural pollen grains as a multifunctional molecular vehicle for functional drug delivery systems and innovative theranostic microdevices.

1. Introduction

Enhanced drug efficacy and molecular targeting of therapeutics have been achieved through delivery systems loaded with multiple drugs as compared with those achieved using delivery systems loaded with a single drug.[1] The strategy of multiple drug loading, which finds wide use in medicinal applications, can also overcome drug resistance and reduce side effects in treatments for cancer and infectious diseases.[2–7] However, conventional multiple molecular loading complicates the process because extra care must be taken to optimize the loading of and preserve the encapsulated drugs.[8,9] The design and construction of stable molecular encapsulation systems using carriers have become pressing issues because many molecules are unstable and thus prone to degradation during transit in biological systems.[10–12] Thus, the protection and the storage of encapsulated molecules in a carrier are challenging and essential for effective drug delivery.

A. K. Prabhakar, M. G. Potroz, S. Park, Prof. N.-J. Cho
School of Materials Science and Engineering
Nanyang Technological University
50 Nanyang Avenue 639798, Singapore
E-mail: NJCHO@ntu.edu.sg
Dr. E. Miyako
Nanomaterials Research Institute (NMRI)
National Institute of Advanced Industrial Science and Technology (AIST)
Central 5, 1-1-1 Higashi, Tsukuba, Ibaraki 305-8565, Japan
E-mail: e-miyako@aist.go.jp

The ORCID identification number(s) for the author(s) of this article can be found under https://doi.org/10.1002/ppsc.201800151.

Plant pollen is one of the most popular natural encapsulants. It can protect the genes and other enclosed biomolecules with its double-layered wall structure composed of cellulosic intine and sporopollenic exine and is produced in copious amounts, which makes it an ideal potential drug delivery platform with various health benefits.[13–16] We have previously used a protein-free microcapsule derivative known as a sporopollenin exine capsule from *Helianthus*[13] and *Lycopodium*[14] for molecular encapsulation purposes. The overall process simplicity and the advantage of high biocompatibility of natural microcapsules from pollens and spores makes them preferred drug carriers. However, ordinary natural encapsulants have demonstrated limited ability to accommodate single-component loads such as proteins and cells.[16]

2. Results and Discussion

2.1. Structural Characterization of Pine Pollen Microcapsule

In the present work, to overcome the problems associated with drug loading in conventional carriers, we developed a dual-molecular loading method utilizing natural pine pollen, which exhibits a bisaccate shape with a core–shell structure and is one of the most industrially active and consumed pollen species (**Figure 1**).[17] This structural uniqueness of pine pollen could impart it with a distinct loading-method-dependent spatial pattern. In this study, five molecular compounds with different sizes and electrical charges were chosen as a therapeutic and diagnostic model to explore their encapsulation behavior into natural pine pollen. The encapsulated molecules were fluorescein-isothiocyanate-labeled bovine serum albumin (FITC-BSA) and FITC-modified immunoglobulin G (IgG) as model therapeutic proteins; Doxorubicin HCl, an anticancer drug; and two organic dyes: Nile Red and Calcein. Simple loading methods namely: passive and vacuum-assisted loading were used with the molecular loading being spatially and quantitatively ascertained. In addition, the structure of BSA molecules in the natural pine pollen was also investigated by circular dichroism (CD) to determine whether pollen can stabilize and protect encapsulated molecules and thereby function as future effective drug delivery systems.
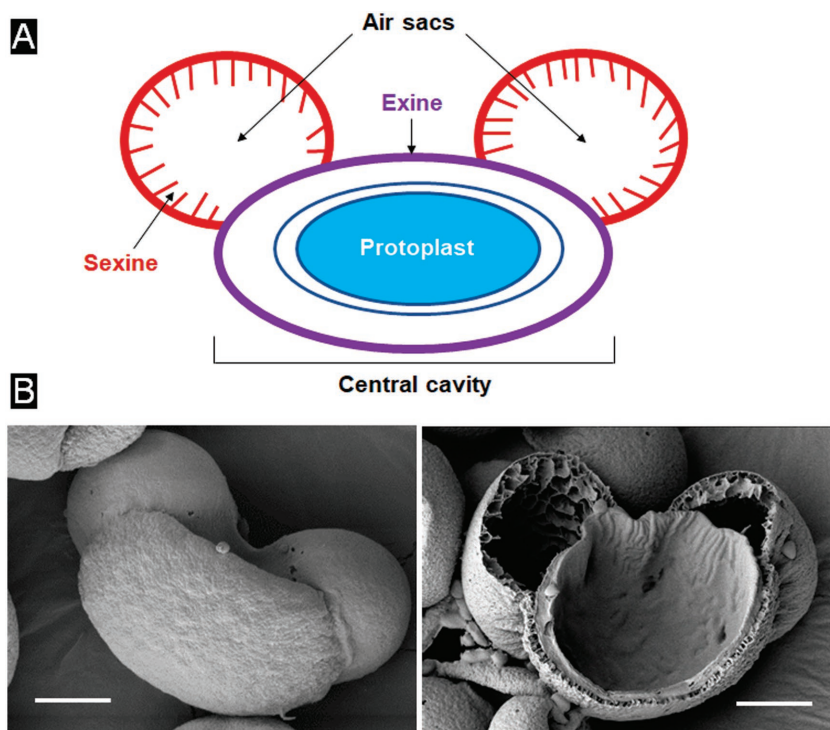
**ADVANCED
SCIENCE NEWS**
www.advancedsciencenews.com

Particle
& Particle Systems Characterization
www.particle-journal.com

Figure 1. A) Schematic of pine pollen structure. B) Scanning electron microscopy (SEM) images of pine pollen (left: whole image, right: cross-section). Scale bars are all 10 µm.

Besides, Bohne et al. dealt with sporopollenin exine capsules (SECs) of pine pollen grains.[18] However, they applied rigorous processing with the use of acids, alkali and organic solvents to purify the pollen grains for their experiments. Herein, we are sure that their permeabilities and surface charge of the SEC themselves are significantly different from natural pine pollen which we use in the current study. In addition, their pine species (*Pinus Sylvestris* and *Pinus Nigra*) are not surely same as ours (*Pinus massoniana*). Thus, I believe that the current study is still unique and furthers knowledge as to molecular encapsulation with natural pine pollen.

2.2. FITC-BSA-Loaded Pine Pollen

First, the molecular loading capability of natural pine pollen was characterized using a single component (FITC-BSA) through confocal laser scanning microscopy (CLSM) (**Figure 2**). We attempted to load FITC-BSA into the pollens using vacuum and passive loading methods individually (see Experimental Section for more details). Interestingly, green fluorescent FITC-BSA was selectively entrapped into the air sac (wing) of pine pollens by the vacuum loading method (100 mbar, 2 h) at an FITC-BSA concentration of 10 mg mL^{-1} (Figures 2A and 1C). In these figures, the blue color originates from pollen autofluorescence and aids in identification of the pollen. Meanwhile, FITC-BSA was not effectively loaded into the pollen via passive loading for 2 h at a FITC-BSA concentration of 10 mg mL^{-1} (Figure 1B,D). In addition, passive loading for longer times and at higher FITC-BSA concentrations (20 mg mL^{-1}) also resulted

in poor uptake even after a long loading duration of 24 h (Figure S1, Supporting Information). The sexine at the surface of the sacci is known to exhibit high permeability toward polymer molecules and latex particles with a diameter of up to 200 nm.[18] In addition, the exine at the central cavity is impermeable to larger molecules (diameter ≥4 nm)[18] for acid-extracted pine microcapsules. Furthermore, applying a vacuum forces the FITC-BSA molecules into the air sacs, facilitating active loading through suction induced by low pressure.[19] Herein, we considered that FITC-BSA is specifically localized and loaded in the air sac of pine pollen in relation to molecular size through forced vacuum loading. Collectively, the results indicate that the vacuum loading method is more effective for compartment-specific targeted loading of BSA molecules into pine pollen microcapsules.

2.3. Pine Pollen Encapsulating Low Molecular Weight Chemical Compounds

Next, other molecules smaller than FITC-BSA (i.e., Doxorubicin HCl, Calcein, and Nile Red) were investigated for their efficiency of encapsulation into the pine pollens to determine whether these molecules exhibit compartmentalization similar to that of FITC-BSA (**Figure 3**). On the basis of the FITC-BSA loading times, vacuum and passive loadings were performed for 2 and 24 h, respectively. Interestingly, all of the molecules were loaded into the central cavity irrespective of the loading method. In fact, Doxorubicin HCl, Nile Red, and Calcein exhibited obvious central cavity loading (strong fluorescence intensity) when loaded by either passive or vacuum loading (Figure 3; Figures S2 and S3, Supporting Information). Table S1 of the Supporting Information summarizes the spatial location of all of the encapsulated molecules depending on the loading method. The larger protein molecules however, were loaded well into the air sacs under vacuum loading and poorly into the central cavity under passive loading.

In particular, Doxorubicin HCl and Nile Red were uniformly encapsulated into the central cavity within 2 h during passive loading (Figure S3, Supporting Information). Negatively charged molecules can electrostatically interact with the protoplast,[20] resulting in attachment sufficiently strong to resist washing. Meanwhile, positively charged molecules such as fuchsine and gentian violet are known to not readily stain pollen grains not subjected to a pollen denaturation process involving an alcohol and acid pretreatment.[21] The overall the loading capacity of Calcein was slightly lower than the capacities of Doxorubicin HCl and Nile Red (Figures S2, Supporting Information). The relatively higher molecular weight of Calcein might be responsible for its exclusion from the central cavity (Table S1, Supporting Information). Consistent with this fact, Calcein appears to be loaded into both the sexine and exine of
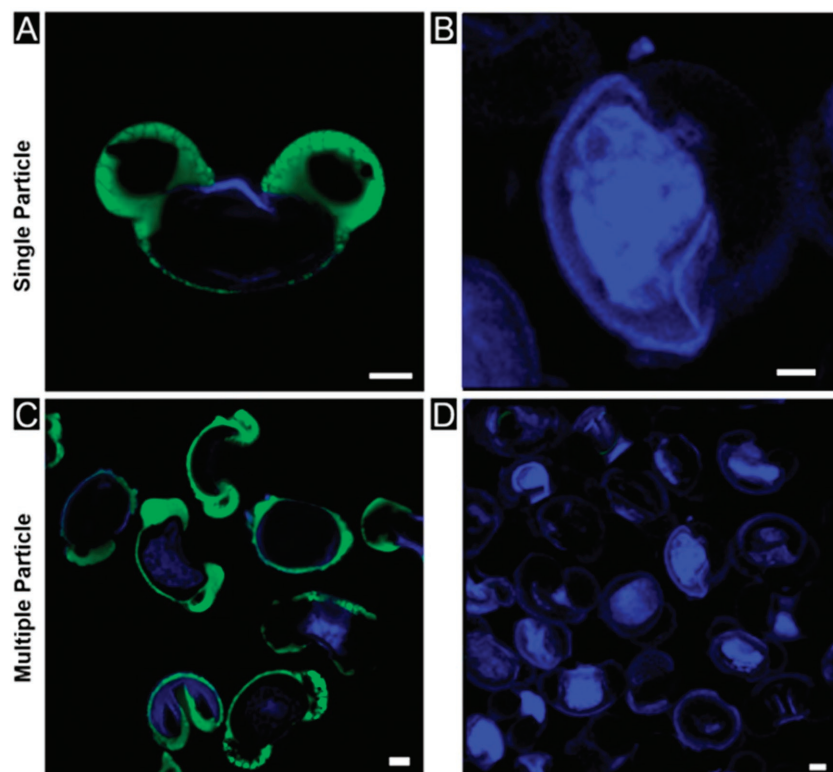
Figure 2. CLSM images of vacuum and passive loading of FITC-BSA into natural pine pollen: Single-particle images of A) a vacuum-loaded sample (10 mg mL^{-1}) and B) a passively loaded sample (10 mg mL^{-1}). Multiple-particle images of C) vacuum-loaded sample (10 mg mL^{-1}) and D) a passively loaded sample (10 mg mL^{-1}). Scale bars are all 10 µm.

mesh and is retained, whereas the smaller ones are washed out. The same behavior was observed for doxorubicin. By contrast, Nile Red, with a size in a similar size range as that of Calcein and Doxorubicin HCl, remained on the sexine and in the central cavity wall even after washing because of its strong lipophilicity.[22] Thus, on the basis of the aforementioned observations, we speculate that a molecule with a size and charge similar to those of FITC-BSA would exhibit compartmentalized loading compared with smaller and positively charged molecules.

2.4. Release Profiles of molecules from Pine Pollen

Our final goal of this research is to build a functional drug delivery system of pollen hybrids via oral administration. Herein, we have calculated the efficiency of loading and amount of released active chemical compounds (Calcein, Doxorubicin HCl, and Nile Red) in addition to BSA molecules (Table S3, Supporting Information). In vitro release profiles of these molecules were monitored in PBS buffer (pH 7) as a model of intestinal environment (Figure S5, Supporting Information). Highly water soluble Calcein, Doxorubicin HCl and BSA molecules were rapidly released from pollen capsules over time, while the hydrophobic Nile Red had a more gradual release pattern, where it released up to 95% in PBS in 1 h (100% release in 24 h) probably because of its water-immiscibility.
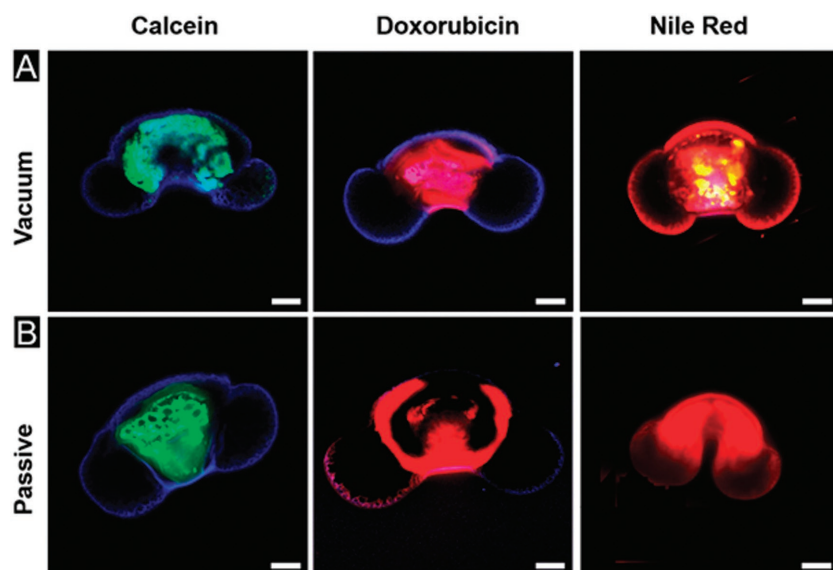
partially washed pollen particles; however, unlike FITC-BSA, no Calcein remained after washing (Figure S4, Supporting Information). This behavior is attributed to the effect of molecular size, where the larger protein is entrapped within the air sac

2.5. Dual-Molecular Loading in Pine Pollen

Combining the vacuum and passive techniques, we next explored dual-molecular loading using FITC-BSA and either Doxorubicin HCl or Nile Red (**Figure 4**). Passive loading for 24 h resulted in the selective loading of Doxorubicin HCl and Nile Red into the central cavity. Thereafter, FITC-BSA preferentially localized in the air sacs after vacuum loading. These results clearly demonstrate that the dual-loading strategy is effective for compartmentalized loading of two distinct types of molecules.

2.6. Encapsulation of Antibody Molecules into Pine Pollen

To extend this unique loading ability to another molecule used in immunotherapy, we subjected IgG[23] to passive loading

Figure 3. CLSM images of natural pine pollen encapsulating Calcein (0.1 mg mL^{-1}), doxorubicin (0.5 mg mL^{-1}), and Nile Red (0.5 mg mL^{-1}), as achieved through A) vacuum loading at 100 mbar for 2 h and B) passive loading for 24 h. Scale bars are all 10 µm.
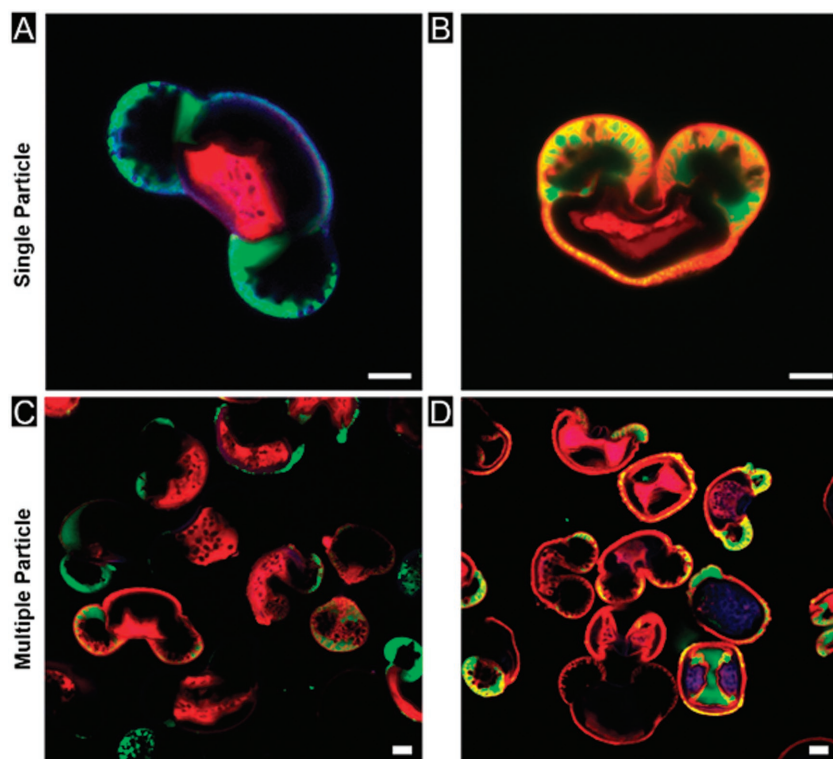
Figure 4. CLSM images of dual-molecule loading into natural pine pollen: single-particle CLSM image of natural pine pollen in which A) doxorubicin and B) (Nile Red) have been encapsulated passively followed by vacuum loading of FITC-BSA. Multiple-particle CLSM images of natural pine pollen in which C) doxorubicin and D) Nile Red have been encapsulated passively followed by vacuum loading of FITC-BSA. Scale bars are all 10 μm.

(10 and 20 mg mL^{-1}) for 24 h. As expected, no loading was observed at either concentration because FITC-IgG is larger than FITC-BSA (**Figure 5**; Figure S6, Supporting Information). Upon vacuum loading (10 mg mL^{-1}), however, air sac loading similar to that of FITC-BSA was observed, where the FITC-IgG was trapped inside the sexine of the air sacs. The spatial localization of FITC-IgG also was similar to that of FITC-BSA, with the sexine layer filling before the inner hollow space, which remained empty because of the impenetrable sexine. This result demonstrates that size plays a major role in the air sac loading and that large proteins can be loaded into natural pine pollen air sacs, whereas small molecules are loaded into the central cavity.

2.7. Structural Preservation of Pine Pollen Encapsulated Protein

A protein's structure is strongly related to its function, and disruption of this structure results in a dysfunctional or non-functional protein.[24] Structure determines the folding of the protein, which exposes its active binding sites and thus makes it functionally active toward binding another protein, enzymatically catalyzing a reaction, etc. Because the BSA is forced into the air sacs, its structure must be ascertained postloading. In the present work, the BSA structure was probed using CD (**Figure 6**).[25] The secondary structure was analyzed preloading and postrelease on the basis of the percent helicity (major

secondary structural element of BSA), which was calculated using ellipticity and was found to be conserved. Specifically, the BSA was found to be 71.03% helical pre-loading and to be 72.29% helical postrelease in PBS. This result indicates that the loading process does not affect the protein structure, which is stably conserved.

3. Conclusion

In summary, we have developed a unique dual-molecular encapsulation method based on natural pine pollen via a simple combination of vacuum and passive loading techniques. Large proteins were loaded into the air sacs of pine pollen through forced vacuum loading, as initially demonstrated with BSA and subsequently confirmed with IgG, whereas passive loading of large proteins was poor. Small dye and drug molecules such as Nile Red, Calcein, and Doxorubicin HCl were loaded through vacuum and passive loadings and were found to localize in the central cavity of the natural pollen particle irrespective of the loading method. These loading phenomena are likely attributable to the size and electrostatic effects of the molecules. Rapid release profiles were observed too with the hydrophilic molecules, while hydrophobic Nile Red displayed a more gradual release profile. The dual-molecular encapsulation showed a compartmentalized loading pattern, enabling doxorubicin or Nile Red to be loaded into the central cavity and FITC-BSA to be loaded into the air sacs via vacuum loading. Even larger IgG molecules were effectively encapsulated into the air sacs of pollen particles by the vacuum loading technique. Furthermore, the protein structure of BSA was shown to be stably conserved on the basis of its helicity determined by CD spectroscopy. Taken together, these techniques represent a simple and robust dual-loading strategy that strongly supports the use of bioinspired natural pine pollen for functional drug delivery and innovative therapeutic microdevices.

4. Experimental Section

Washing of Natural Pine Pollen: Natural pine pollen (30 g) from *Pinus massoniana* was vacuum filtered four times (1 L of distilled water each) to remove dust and other smaller plant debris and was then vacuum filtered through a 100 μm nylon mesh to separate the larger fibers from the smaller pollen particles. The pollen was then freeze-dried to obtain clean and dry natural pine pollen.

Surface Morphology Evaluation by Scanning Electron Microscopy (SEM): SEM imaging was performed using a JSM 5410 (JEOL, Tokyo, Japan). Samples were sputter-coated using a JFC-1600 instrument (JEOL, Tokyo, Japan) (20 mA, 60 s) to obtain a 10 nm thick gold film. Images were captured at an accelerating voltage of 5 kV at different magnifications. For particle cross-sections, particles were adhered to carbon tape, submerged in liquid nitrogen for ≈20 s, and then cut across the adhered
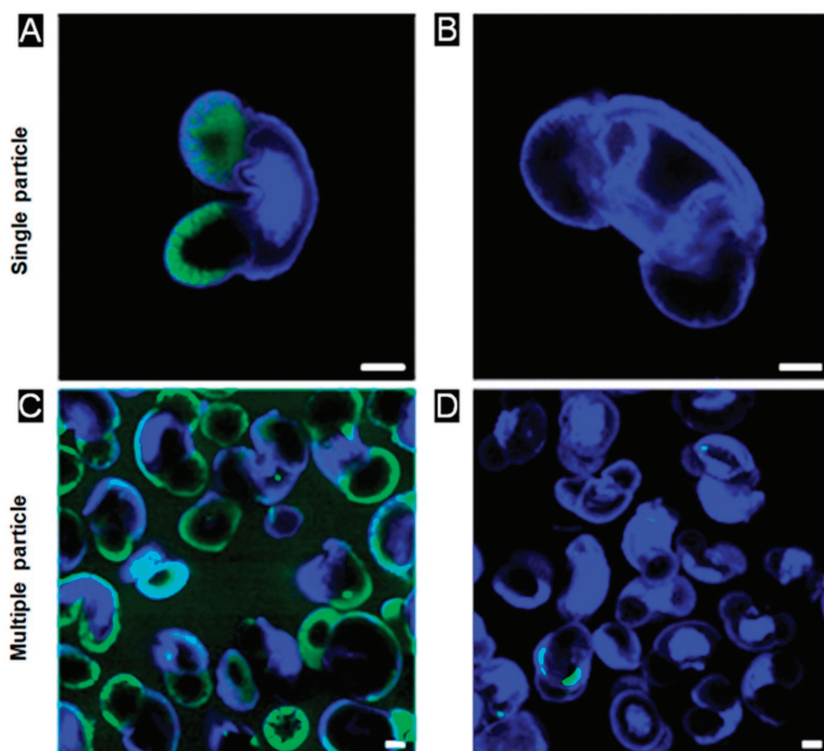
ADVANCED
SCIENCE NEWS
www.advancedsciencenews.com

Particle
& Particle Systems Characterization
www.particle-journal.com

Figure 5. Single-particle CLSM images of A) vacuum-loaded FITC-IgG (10 mg mL^{-1}) and B) passively loaded FITC-IgG (20 mg mL^{-1}). Multiple-particle CLSM images of C) vacuum-loaded FITC-IgG (10 mg mL^{-1}) and D) passively loaded FITC-IgG (20 mg mL^{-1}). Scale bars are all 10 µm.

pollen multiple times with a scalpel blade. Cross-sectioned particles were identified by examining cut marks during imaging.

Confocal Laser Scanning Microscopy Analysis: Protein, drug, and dye-loaded natural pine pollen samples were mounted onto sticky slides with Vectashield and scanned via CLSM (Carl Zeiss LSM700, Germany). Laser excitation lines were set to 405, 488, and 561 nm at a scan speed of 67 s per phase. Images were collected with differential interference contrast at 405 nm (6.5%), 488 nm (6%), and 561 nm (6%) using enhanced-contrast Plan-Neofluar 20×, 40×, and 63× oil-objective M27 lenses. The fluorescence emission was collected in photomultiplier
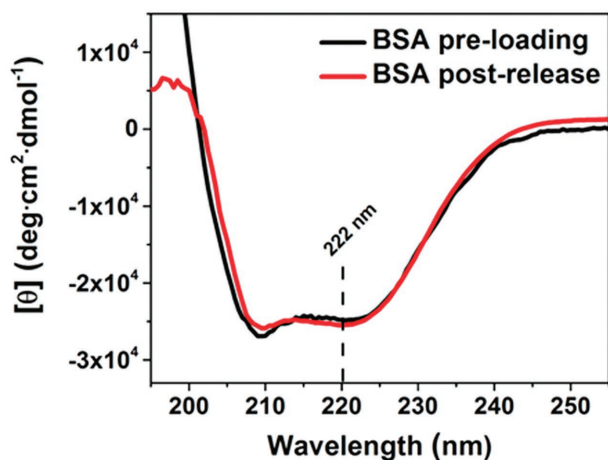

Figure 6. Circular dichroism spectra of native BSA before encapsulation and BSA postrelease in PBS for 15 min.

tubes equipped with different filters (416–477, 498–550, and 572–620 nm) and analyzed using the ZEN software (Carl Zeiss, Germany).

Passive Loading: Natural pine pollen (10 mg) was mixed with 200 µL of FITC-BSA (10 or 20 mg mL^{-1}), Calcein (0.1 mg mL^{-1}), Doxorubicin HCl (0.5 mg mL^{-1}), Nile Red (1 mg mL^{-1}), and FITC-IgG (20 mg mL^{-1}). The resultant mixtures were placed on a shaker and shaken at 500 rpm for 24 h, after which they were washed with suitable solvents and observed by CLSM.

Vacuum Loading: Natural pine pollen (10 mg) was mixed with 200 µL of FITC-BSA (10 mg mL^{-1}), Calcein (0.1 mg mL^{-1}), Doxorubicin HCl (0.5 mg mL^{-1}), Nile Red (1 mg mL^{-1}), or FITC-IgG (10 mg mL^{-1}), and the samples were subjected to a vacuum of 100 mbar for 2 h. They were then washed with suitable solvents and examined by CLSM.

Dimensions and Zeta Potential: All dimensions were estimated using the Draw ProteinDimensions plugin in Pymol using PDB or chemical files. The zeta potential of all of the encapsulates [FITC-BSA (10 mg mL^{-1}), Calcein (0.1 mg mL^{-1}), Doxorubicin HCl (0.5 mg mL^{-1}), Nile Red (1 mg mL^{-1}), and FITC-IgG (10 mg mL^{-1})] was measured using a Zeta Cell (DTS-1070) with 1 mL of solution.

Dual-Molecular Loading: For passive loading, natural pine pollen (10 mg) was added separately to 200 µL of Doxorubicin HCl (1 mg mL^{-1}) and Nile Red (0.5 mg mL^{-1}) both separately, followed by washing. 1 mL of FITC-BSA (10 mg mL^{-1}) was then added, and the resultant mixture was subjected to vacuum loading at 100 mbar for 2 h, after which the formulation was washed and observed by CLSM.

Calculation of Loading Efficiency: Natural pine pollen (50 mg) was mixed with 2 mL of FITC-BSA (10 mg mL^{-1}), Calcein (0.1 mg mL^{-1}), Doxorubicin HCl (2.5 mg mL^{-1}), and Nile Red (0.1 mg mL^{-1}) all separately and the samples were subject to a vacuum of 100 mbar for 2 h after which they were washed with solvents (water or ethanol), freeze-dried, and estimated for their loading efficiencies from their individual calibration curves using the UV spectrophotometer (Boesco-S220, Germany) and the below formula

$$BSA\ loading\ (\%) = \frac{Weight\ of\ encapsulated\ BSA}{Weight\ of\ BSA\text{-loaded pollen powder}} \times 100 \quad (1)$$

The theoretical maximum corresponds to 100% loading of the molecules into the feed mass of pollen (50 mg).

Molecular Release from Natural Pine Pollen: 10 mg of the above loaded formulations were immersed in PBS (20% ethanol for Nile Red alone) with suitable blanks (unloaded natural pine pollen) with 1 mL of solution taken out at different time points and replaced with fresh solution. Finally, release profiles were calculated from the respective calibration curves using the UV spectrophotometer.

BSA Loading and Release into Natural Pine Pollen for CD: 100 mg of pollen was mixed with 2 mL of 50 mg mL^{-1} of BSA, and the mixture was vortexed for 5 s followed by vacuum loading at 100 mbar for 2 h, after which it was washed. This procedure was conducted in triplicate. 55 mg of the aforementioned formulation was dissolved in 1 mL of PBS (pH 7) to give a final BSA concentration of 8.72 µm after 15 min. Pure BSA diluted to a concentration of 11 × 10^{-6} M was used as a preloading reference sample for CD. The release of BSA from natural pine pollen also released protein from pine pollen; thus, a solution containing protein from natural pine pollen was used as the blank for estimating the postrelease secondary structure.

CD Analysis: The secondary structure of the presented proteins was characterized by CD using a Chriascan spectropolarimeter (model 420,

ADVANCED
SCIENCE NEWS
www.advancedsciencenews.com

Particle
& Particle Systems Characterization
www.particle-journal.com

AVIV Biomedical Inc.) with cuvette with a 0.01 cm path length (Hellma). The concentration of all of the prepared samples was measured by UV spectrophotometry (Boesco-S220, Germany) at 280 nm. Spectral data were collected in triplicate at 25 °C over the wavelength range from 190 to 260 nm with 1 nm bandwidth, a step size of 0.5 nm, and a time constant of 0.1 s. Baseline scans were recorded using the same parameters as those used for the protein solvent (PBS or natural pine pollen protein in PBS) and were subtracted from the corresponding data scans with protein samples. The final corrected averaged spectra were expressed in mean residue molar ellipticity ([θ]), and the presented spectra were smoothed by the Savitzky–Golay method. The fractional helicity (fH) of the peptides was calculated as follows[26]

$$fH = \left([\theta]_{222}^{Obs} - 3000 \right) / \left(-36000 - 3000 \right) \qquad (2)$$

where $[\theta]_{222}^{Obs}$ is the molar ellipticity at 222 nm

Supporting Information

Supporting Information is available from the Wiley Online Library or from the author.

Acknowledgments

Conflict of Interest

The authors declare no conflict of interest.

Keywords

[1] a) J. N. Lockhart, D. M. Stevens, D. B. Beezer, A. Kravitz, E. Harth, *J. Controlled Release* **2015**, *220*, 751; b) W. Scarano, P. de Souza, M. H. Stenzel, *Biomater. Sci.* **2015**, *3*, 163; c) S. Wu, X. Yang, Y. Lu, Z. Fan, Y. Li, Y. Jiang, Z. Hou, *Drug Delivery* **2017**, *24*, 51.

[2] E. M. Shapiro, S. Skrtic, K. Sharer, J. M. Hill, C. E. Dunbar, A. P. Koretsky, *Proc. Natl. Acad. Sci. USA* **2004**, *101*, 10901.

[3] Y. Y. Hui, W. W.-W. Hsiao, S. Haziza, M. Simonneau, F. Treussart, H.-C. Chang, *Curr. Opin. Solid State Mater. Sci.* **2017**, *21*, 35.

[4] L. Accomasso, C. Gallina, V. Turinetto, C. Giachino, *Stem Cells Int.* **2015**, *2016*, 7920358.

[5] a) A. Fernandez-Fernandez, R. Manchanda, A. J. McGoron, *Appl. Biochem. Biotechnol.* **2011**, *165*, 1628; b) S. S. Kelkar, T. M. Reineke, *Bioconjugate Chem.* **2011**, *22*, 1879.

[6] B. Zhou, Y. Li, G. Niu, M. Lan, Q. Jia, Q. Liang, *ACS Appl. Mater. Interfaces* **2016**, *8*, 29899.

[7] a) J. V. Jokerst, S. S. Gambhir, *Acc. Chem. Res.* **2011**, *44*, 1050; b) P. J. Kempen, S. Greasley, K. A. Parker, J. L. Campbell, H.-Y. Chang, J. R. Jones, R. Sinclair, S. S. Gambhir, J. V. Jokerst, *Theranostics* **2015**, *5*, 631; c) R. Shahbazi, B. Ozpolat, K. Ulubayram, *Nanomedicine* **2016**, *11*, 1287; d) M. K. Yu, J. Park, S. Jon, *Theranostics* **2012**, *2*, 3.

[8] Q. Hu, W. Sun, C. Wang, Z. Gu, *Adv. Drug Delivery Rev.* **2016**, *98*, 19.

[9] a) M. Magnani, L. Rossi, M. D'ascenzo, I. Panzani, L. Bigi, A. Zanella, *Biotechnol. Appl. Biochem.* **1998**, *28*, 1; b) M. Delcea, N. Sternberg, A. M. Yashchenok, R. Georgieva, H. Bäumler, H. Möhwald, A. G. Skirtach, *ACS Nano* **2012**, *6*, 4169.

[10] B. Garcia-Moreno, *Proteins: Structure, Function, and Bioinformatics*, Wiley-VCH, Weinheim, Germany **2017**.

[11] W. Wang, C. J. Roberts, *Aggregation of Therapeutic Proteins*, Wiley-VCH, Weinheim, Germany **2010**.

[12] V. P. Souza, C. M. Ikegami, G. M. Arantes, S. R. Marana, *FEBS J.* **2016**, *283*, 1124.

[13] R. C. Mundargi, M. G. Potroz, S. Park, H. Shirahama, J. H. Lee, J. Seo, N. J. Cho, *Small* **2016**, *12*, 1167.

[14] R. C. Mundargi, M. G. Potroz, S. Park, J. H. Park, H. Shirahama, J. H. Lee, J. Seo, N. J. Cho, *Adv. Funct. Mater.* **2016**, *26*, 487.

[15] a) R. C. Mundargi, M. G. Potroz, J. H. Park, J. Seo, J. H. Lee, N.-J. Cho, *RSC Adv.* **2016**, *6*, 16533; c) R. C. Mundargi, M. G. Potroz, J. H. Park, J. Seo, E. L. Tan, J. H. Lee, N. J. Cho, *Sci. Rep.* **2016**, *6*, 19960; d) J. H. Park, J. Seo, J. A. Jackman, N. J. Cho, *Sci. Rep.* **2016**, *6*, 28017.

[16] a) S. M. Alshehri, H. A. Al-Lohedan, A. A. Chaudhary, E. Al-Farraj, N. Alhokbany, Z. Issa, S. Alhousine, T. Ahamad, *Eur. J. Pharm. Sci.* **2016**, *88*, 158; b) S. Barrier, A. S. Rigby, A. Diego-Taboada, M. J. Thomasson, G. Mackenzie, S. L. Atkin, *LWT – Food Sci. Technol.* **2010**, *43*, 73; c) A. Diego-Taboada, S. T. Beckett, S. L. Atkin, G. Mackenzie, *Pharmaceutics* **2014**, *6*, 80; d) S. A. Hamad, A. F. K. Dyab, S. D. Stoyanov, V. N. Paunov, *J. Mater. Chem.* **2011**, *21*, 18018.

[17] S. H. Buhner, *Pine Pollen: Ancient Medicine for a New Millennium*, BookBaby, Pennsauken, NJ, USA **2012**.

[18] G. Bohne, E. Richter, H. Woehlecke, R. Ehwald, *Ann. Bot.* **2003**, *92*, 289.

[19] M. G. Potroz, R. C. Mundargi, J. J. Gillissen, E. L. Tan, S. Meker, J. H. Park, H. Jung, S. Park, D. Cho, S. I. Bang, *Adv. Funct. Mater.* **2017**, *27*, 1700270.

[20] C.-N. Huang, M. J. Cornejo, D. S. Bush, R. L. Jones, *Protoplasma* **1986**, *135*, 80.

[21] a) D. H. Heilman, H. W. Bernton, D. L. Dunner, S. M. Barber, *Stain Technol.* **1963**, *38*, 193; b) M. P. Alexander, *Stain Technol.* **1980**, *55*, 13; c) C. A. Brown, *Grana* **1958**, *1*, 39; d) D. Festi, D. L. Hoffmann, M. Luetscher, *Quat. Res.* **2016**, *86*, 45.

[22] P. Greenspan, E. P. Mayer, S. D. Fowler, *J. Cell Biol.* **1985**, *100*, 965.

[23] a) A. Gardulf, U. Nicolay, *Curr. Opin. Allergy Clin. Immunol.* **2006**, *6*, 434; b) V. Irani, A. J. Guy, D. Andrew, J. G. Beeson, P. A. Ramsland, J. S. Richards, *Mol. Immunol.* **2015**, *67*, 171; c) A. Saxena, D. Wu, *Front. Immunol.* **2016**, *7*, 580; d) Y. Mimura, T. Katoh, R. Saldova, R. O'Flaherty, T. Izumi, Y. Mimura-Kimura, T. Utsunomiya, Y. Mizukami, K. Yamamoto, T. Matsumoto, *Protein Cell* **2017**, *9*, 47.

[24] a) P. Ascenzi, A. Bocedi, M. Marino, *Mol. Aspects Med.* **2006**, *27*, 299; b) H. Hegyi, M. Gerstein, *J. Mol. Biol.* **1999**, *288*, 147; c) S. Nakai, *J. Agric. Food Chem.* **1983**, *31*, 676.

[25] S. M. Kelly, N. C. Price, *Curr. Protein Pept. Sci.* **2000**, *1*, 349.

[26] J. D. Morrisett, J. S. David, H. J. Pownall, A. M. Gotto Jr., *Biochemistry* **1973**, *12*, 1290.